Spatial and Temporal Characteristics of 60-GHz Indoor Channels

Hao Xu, *Member, IEEE*, Vikas Kukshya, *Member, IEEE*, and Theodore S. Rappaport, *Fellow, IEEE*

***Abstract*—This article presents measurement results and models for 60-GHz channels. Multipath components were resolved in time by using a sliding correlator with 10-ns resolution and in space by sweeping a directional antenna with 7° half power beamwidth in the azimuthal direction. Power delay profiles (PDPs) and power angle profiles (PAPs) were measured in various indoor and short-range outdoor environments. Detailed multipath structure was retrieved from PDPs and PAPs and was related to site-specific environments. Results show an excellent correlation between the propagation environments and the multipath channel structures. The measurement results confirm that the majority of the multipath components can be determined from image based ray tracing techniques for line-of-sight (LOS) applications. For non-LOS (NLOS) propagation through walls, the metallic structure of composite walls must be considered. From the recorded PDPs and PAPs, received signal power and statistical parameters of angle-of-arrival and time-of-arrival were also calculated. These parameters accurately describe the spatial and temporal properties of millimeter-wave channels and can be used as empirical values for broadband wireless system design for 60-GHz short-range channels.**

***Index Terms*—Angular spread, delay spread, fading, millimeter-wave propagation, multipath channels, space time channel models.**

I. Introduction

ADVANCED wireless systems exploit dimensions of time, frequency, and space to maximize the data rate and system capacity. Design of space-time coding, equalization, adaptive antennas, and rake receiver techniques relies on accurate characterization of the propagation channel. Classical channel models were developed for narrowband systems [1], [2]. For wireless systems with high data rates and directional antennas, the small-scale fading is more complex to characterize than for omnidirectional and narrowband systems of the past. More advanced channel models which include time dispersion and angular dispersion have also been developed [3], [4].

The work presented in this paper focuses on characterization of 60-GHz channels both in space and time delay. The 60-GHz spectrum has been proposed for future-generation broad-band wireless systems in indoor and short-range outdoor environments. In the U.S., as much as 5 GHz (from 59 to 64 GHz) is in license-free spectrum. In practice, site-specific prediction techniques, such as ray tracing, are used to model millimeter-wave channels [5]. However, little literature is available to carefully verify the ray-tracing model with high-resolution measurements or to provide detailed angle-of-arrival (AOA) and time-of-arrival (TOA) parameters for the 60-GHz channels.

The goal of this research is threefold.

- accurately measure the channel multipath structure by separating multipath components by their AOAs and TOAs;
- determine the origin of multipath by relating multipath AOA and TOA to site-specific information;
- provide practical values of statistical AOA and TOA parameters for various propagation environments, so the empirical results may be replicated by simulators [6].

Section II presents the experimental setup for the channel measurements. Section III relates the measured channel responses to the propagation environments. Section IV describes the measured AOA and TOA parameters and Section V summarizes this work.

II. Measurement Setup

A. Methods to Separate Multipath Components

Multipath components can be classified either by their AOA or TOA. The corresponding channel characteristics can be recorded as a *power delay profile* (PDP) or a *power angle profile* (PAP). A PDP records temporal power distribution relative to multipath TOA and a PAP records spatial power distribution relative to multipath AOA. Wideband measurement techniques, such as a vector network analyzer or sliding correlator, are used to resolve multipath by their delay times. However, all measurement systems use a band-limited probing waveform and thus have limited time resolution. Even with the 10-ns resolution used in this measurement campaign, the received signal pulse may still contain several multipath components and thus may fade in a small local area. One method for decreasing local fading while increasing multipath resolution is to use directional antennas at the receiver to separate multipath by space, provided that they arrive from different directions.

Angular separation of multipath components can be achieved by using direction-finding antenna arrays [7], synthetic aperture radar technique [8]–[10], or highly directional antennas [11], [12]. In *antenna array systems*, multiple antennas are used at the receiver. Signals received at the array elements are weighted and combined to attenuate received signals arriving from outside the desired spatial direction. This technique allows fast measurements of the channel but is prone to mutual coupling among

Manuscript received March 19, 2001; revised September 13, 2001. This paper was supported in part by HRL Laboratories. This work was presented at the IEEE VTC, Boston, MA, September 24–28, 2000.

H. Xu is with Wireless Communications Research Department, at Bell Laboratories, Lucent Technologies, Holmdel, NJ 07733 USA (e-mail: haoxu@lucent.com).

V. Kukshya and T. S. Rappaport are with the Mobile and Portable Radio Research Group, Bradley Department of Electrical and Computer Engineering, Virginia Polytechnic Institute and State University, Blacksburg, VA 24061 USA (e-mail: wireless@vt.edu).

Publisher Item Identifier S 0733-8716(02)04408-6.

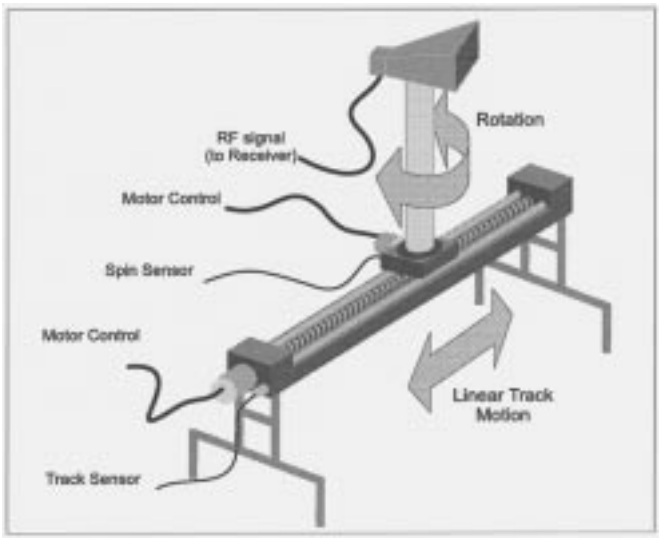

Fig. 1. Automated track system [13].

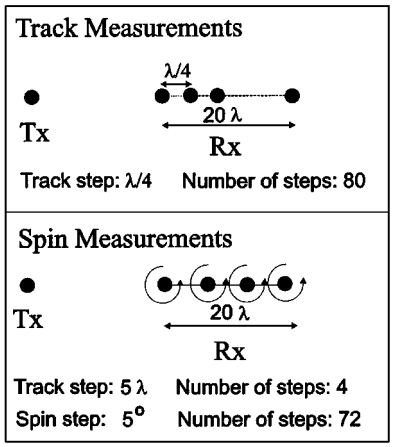

Fig. 2. Track and spin measurement procedure.

antenna elements and requires a large number of antenna elements to obtain substantial spatial resolution. *Synthetic aperture radar techniques* eliminate mutual coupling by using only one antenna that moves into different locations of the array. It produces results similar to an antenna array, provided all measurements are taken within the channel's coherence time. Electronic beamforming techniques, such as direction-finding antenna arrays, require accurate phase measurements and elaborate processing. PAPs can also be measured by mechanically rotating a *highly directional antenna*. The advantage of mechanically rotating a directional antenna is that no phase information is required to accomplish beam steering. At low frequencies, highly directional antennas have large physical dimensions and present difficulty in mechanical steering. However, at millimeter wave frequencies, miniaturized directional antennas with large gains are small and can be easily rotated.

B. Measurement Procedure

In this measurement campaign, a mechanically steered directional antenna was used to resolve multipath components. An automated system was used to precisely position the receiver antenna along a linear track and then rotate the antenna in the azimuthal direction. The track system is shown in Fig. 1. The precisions of the track and spin positions are less than 1 mm and 1°, respectively [13]. When a highly directional antenna is used, the system provides high spatial resolution to resolve multipath components with different AOAs. The sliding correlator technique was used to further resolve multipath components with the same AOA by their TOAs. The spread spectrum signal had a RF bandwidth of 200 MHz, which provided a time resolution of approximately 10 ns.

To measure and model different propagation environments, the measurements were taken in various locations (site information is described in Section II-D). At each location, both *track measurements* and *spin measurements* were performed as shown in Fig. 2.

- Track measurements: During a track measurement, the transmitter and receiver antennas are pointed directly at each other and the receiver is moved along the track aligned with the LOS path. PDPs are taken at 80 positions along the track with a separation of a quarter wavelength. This allows a spatial sampling rate of four samples per wavelength along the track with a length of 20 wavelength. The purpose of the track measurements is to study the range of small-scale signal variations of each resolvable multipath component, as well as TOA statistics for typical indoor applications, where transmitter and receiver antennas are fixed and aligned on bore sight.
- Spin measurements: During a spin measurement, the receiver is moved along the linear track to four different positions. The spatial separation between two successive positions is five wavelengths. At each position, the receiver antenna is rotated in azimuth from 0° to 360° with a step size of 5° and PDPs are recorded at each of the 72 angular steps. Then, a local average is calculated from the measurement results at four different positions. The local average helps to remove any residual small-scale or time-varying fading that may occur at individual positions. The averaged PDPs and PAPs are processed to obtain the AOA and TOA statistics of the channel. Definitions of the statistical parameters are presented in Section IV-A and the measurement results are presented in Section IV-B. The purpose of the spin measurement is to obtain the complete spatial-temporal characteristics of the channel. The general results provide deep understanding of the wave propagation in a local area. The measured results can also be applied to verification of ray tracing channel estimation, position location algorithms, and statistical channel models for both fixed and mobile indoor wireless applications.

C. Antenna Patterns

For this measurement campaign, an open-ended waveguide with 6.7-dB gain was used as the transmitter antenna and a horn antenna with 29-dB gain was used as the receiver antenna. These antennas were chosen to emulate typical antenna systems that have been proposed for millimeter-wave indoor applications, where a sector antenna is used at the transmitter and a highly directional antenna is used at the receiver. Both antennas are

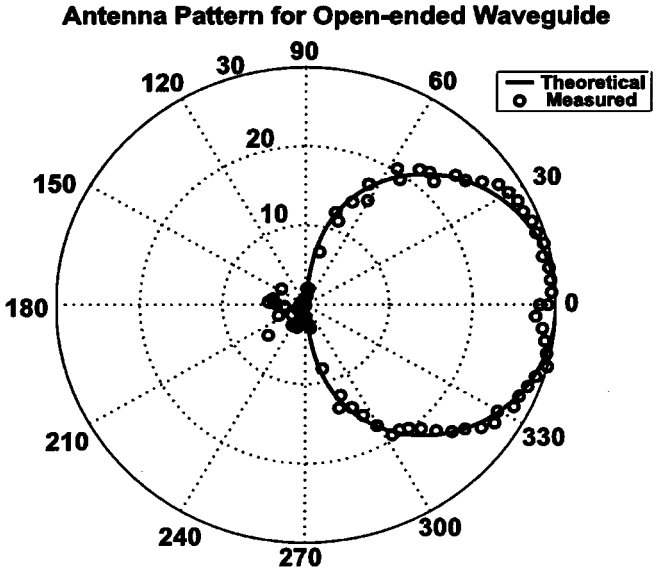

Fig. 3. Theoretical and measured antenna patterns for the open-ended waveguide.

vertically polarized and mounted on adjustable tripods about 1.6 m above the ground. The theoretical half power beamwidths (HPBW) are 90° in azimuth and 125° in elevation for the open-ended waveguide and 7° in azimuth and 5.6° in elevation for the horn antenna.

The antenna patterns were measured by sweeping the antenna under test in an empty parking lot and plotting the peak received power at each pointing angle. In order to reduce the potential effects of measurement noise, this spin measurement was repeated four times for each antenna to generate an averaged antenna pattern. As an example, the measured and theoretical antenna patterns for the open-ended waveguide are presented in Fig. 3. The theoretical pattern is based on the E-field integration method and it produces an accurate H-plane pattern in the front hemisphere [14]. The measured antenna pattern agrees well with the theoretical prediction in the front hemisphere. As the measurements show, the leakage into the back hemisphere is negligible (at least 25 dB below the peak power).

D. Site Description

A total of 33 spin and track measurements in eight different locations were measured on the Virginia Tech campus. Locations 1 and 2 were typical building hallways. Location 1 was in the hallway on the forth floor of Durham Hall. Durham Hall is a four-story concrete building, which was built in 1997. The hallway dimensions are $102 \times 2.1 \times 4.3$ m. (In this section, all the dimensions are given in the order of length, width, and height.) Location 2 was the hallway on the second floor of Whittemore Hall. The hallway dimensions are $54.7 \times 2.9 \times 4.3$ m. For both locations, the transmitter was fixed at one end of the hallway. Several receiver positions were chosen at separations ranging from 5 to 60 m from the transmitter. All receiver positions had LOS to the transmitter.

Locations 3 and 4 were in small to medium-sized rooms. Location 3 was in a conference room on the forth floor of Durham Hall. The dimensions of the room are $6.7 \times 5.9 \times 4.3$ m. The transmitter was fixed in one corner of the room. The receiver was placed in two different positions: in the opposite corner of the room and the center of the room. Location 4 was in a classroom in Whittemore Hall with dimensions of $8.4 \times 7.1 \times 4.3$ m. The transmitter was fixed in one corner of the room. The receiver was placed in four different positions: the center and the other three corners of the room.

Locations 5 and 6 were chosen to study NLOS propagation from a hallway to a room and from a room to an adjacent room, respectively. In location 5, the receiver was in a laboratory with dimensions of $11.7 \times 5.1 \times 4.3$ m. The transmitter was placed in the hallway. Two different positions were measured. In one position, the transmitter and receiver antennas were separated by a plasterboard wall with metallic studs inside. In the other position, the antennas were separated by the glass door. In location 6, the transmitter and receiver were placed in two adjacent rooms separated also by a plasterboard wall with metallic studs inside. The dimensions of the rooms are $11.7 \times 5.1 \times 4.3$ m and $5.1 \times 4.3 \times 4.2$ m. For both walls, the metallic studs are separated by 40 cm (16 in).

Locations 7 and 8 were outdoor locations. Location 7 was in a parking lot with no cars. The only possible scatterers were the lamp posts. This location was selected to perform free-space calibration and antenna pattern measurements. Location 8 was near the exterior stone wall of Durham Hall. The transmitter and receiver were placed along the wall with a separation of 2 to 5 m between the antennas. Both antennas were 3.5 m from the wall. The simple propagation environments of locations 7 and 8 were chosen to verify the system performance.

The main rationale of choosing these eight locations was to provide a variety of different propagation scenarios for the measurements and also to provide controllable environments for analysis and site-specific channel modeling.

III. Relating Multipath Structure to Propagation Environments

A. Power Angle Profiles

This section investigates the correlation between the propagation environments and the multipath AOA. Measured PAPs are imported into the site-map to identify the origin of each multipath component.

Examples of the received PAP results are shown in Fig. 4 for propagation within a room, in Fig. 5 for propagation in a hallway, and in Fig. 6 for propagation into rooms.

The PAPs exhibit strong correlation with the propagation environment. The following observations were made from the recorded PAPs.

- *Propagation within a room*: As shown in Fig. 4, when an LOS path exists, the strongest multipath component is always from the LOS direction. The value of the maximum multipath power is given as P in decibels per meter in the legend. Powers of the other small multipath components are given in decibels in the polar plots in the figure relative to the maximum power. LOS and the first-order reflected waves contribute the majority of the multipath components (the order of reflection refers to the number of reflections that a multipath component goes through before

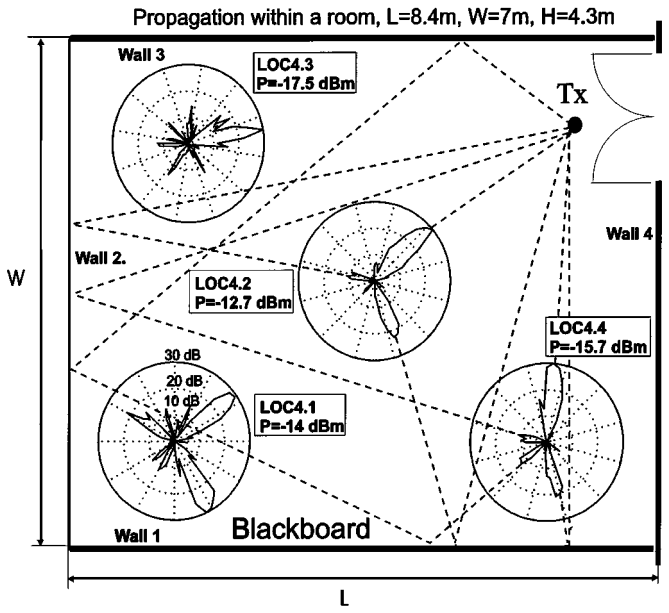

Fig. 4. AOA measurements for propagation within a room (location 4), relative power levels shown on polar plots, and peak multipath power (P) given in text. Rays are shown only for locations 4.2 and 4.4 in the figure, although a similar procedure can be performed for all the locations.

it reaches the receiver). For example, in the center location 4.2 (as shown in Fig. 4), there are only three strong multipath components: one is the LOS component, the other two are first-order reflected waves from the side walls. The reflected wave from "wall 2" is 19 dB below the LOS component. The blackboard appears to be a strong reflector. The reflected wave from the blackboard is only 8 dB below the LOS path. There are more multipath components received in the corner locations of the room. In location 4.4, the multipath components consist of LOS component, first-order reflected waves from "wall 2" and the blackboard, and the second-order reflected wave from "wall 2" and the blackboard. Similar analysis was performed for locations 4.1 and 4.3. At location 4.1, the strong reflection of the blackboard resulted in a multipath component with comparable power as the LOS component.

- *Propagation in a hallway*: Fig. 5 shows the measurement results of location 2 in the hallway. For all the measurement positions, the strongest multipath component came from the LOS direction. For location 2.1, the main multipath components are LOS and the reflected waves from the sidewalls. Location 2.2 is near the intersection of two hallways. The LOS component and reflected waves from sidewalls are still strong but became more diffusive. A strong multipath component came from the corner of room 257. As shown in locations 2.3, 2.4, and 2.5, when the separation further increases, the reflections from the sidewalls became insignificant. The reflection from the other end of the hallway became stronger. Results from location 2.5 clearly show the LOS and the reflected wave components.

  Note that with the increase of the separation distance, the reflected wave components from the floor or ceiling can become significant. The strength of the reflected wave depends on the antenna beamwidth, antenna polarization, antenna heights, the hallway geometry, and the dielectric properties of the reflecting surfaces. Results from [17] show that, at 60 GHz, the reflection coefficient for typical floor is roughly 0.3 for incident angles less than 10°. Using this result and our measurement setup, the estimated power of the reflected wave from the floor is at least 16 dB and 14 dB below the LOS component at separations of 50 m and 60 m, respectively. When the receiver antenna is sweeped in azimuth, these reflected waves are added to the LOS power at zero degree of AOA. The effects of these reflected waves are thus negligible. At distances less than 50 m, the effects are even smaller.
- *Propagation through walls*: Fig. 6 shows the measurement results for NLOS propagation into rooms. In both locations, the radio wave propagates through a composite wall with metallic studs. Results indicate that the metallic studs have strong impact on the millimeter-wave propagation. In location 5, the metallic studs do not obstruct the LOS path. Measurement results show that the penetration loss is 9 dB through the wall between the room and the hallway. The strongest multipath component is still from the transmitter direction. Other major multipath components are reflected waves from the metallic bookshelves. The multipath energy seems to be more diffuse in their AOAs in this NLOS case as compared to the LOS propagation within a room (Fig. 4). Reflections/scattering of the radio wave from the studs also contribute to the multipath components.

  In location 6, the metallic stud obstructs the LOS path and the measurement results show that the penetration loss through the wall and the blackboard is as high as 35.5 dB. Since the LOS path was highly attenuated, the maximum multipath power is assumed to be from the reflected path through two glass doors. Other strong multipath components might come from scattering from the large plotter or the studs in the wall.

  It is interesting to note that not all the reflections from the metallic studs are significant. In Fig. 6, for example, only studs on the left side of the LOS path resulted in strong reflections. This is due to the shape of the metallic stud as shown in Fig. 6. Only the wave impinging on the smooth side of the stud results in strong reflections.

These measurement results clearly demonstrate a strong correlation between the propagation environments and the multipath channel structure. The following general conclusions can be made from all the measurement results.

- For LOS applications, free space propagation and reflection are the dominant propagation mechanisms. When there are no strong reflectors in the propagation environment, the reflected multipath components are at least 10 dB below the LOS component. LOS component and first-order reflected waves contribute a majority of the received signal power. Strong multipath components can result from strong reflectors, such as metallic furniture. When strong reflectors are present, the reflected wave can be comparable to the LOS component. Image-based ray tracing can be used to estimate the channel multipath structure at millimeter-wave frequencies. For installation purposes or a rule-of-thumb estimation, LOS and

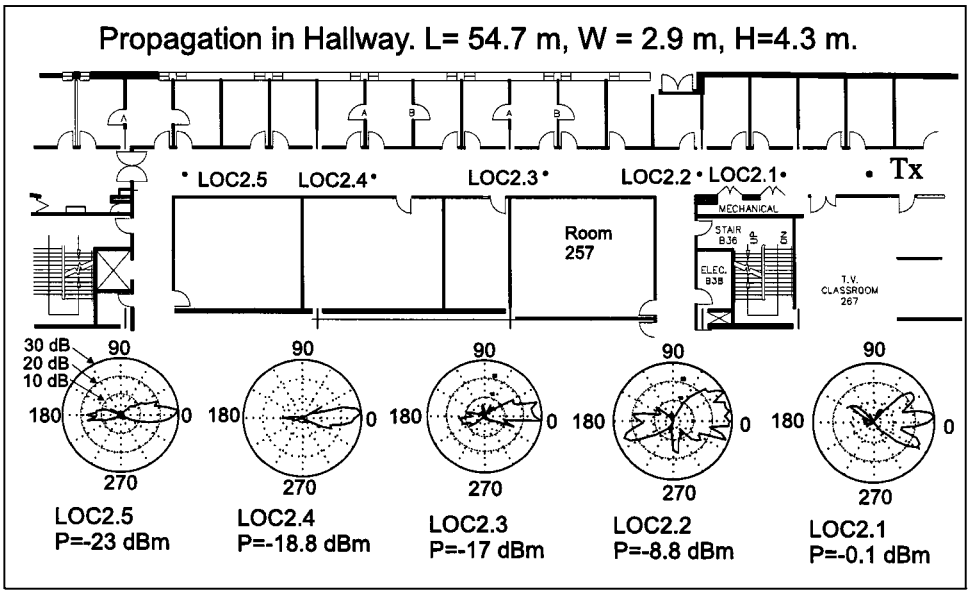

Fig. 5. AOA measurements for propagation along a hallway (location 2), relative power levels given in polar plots, and peak multipath power (P) given in text.

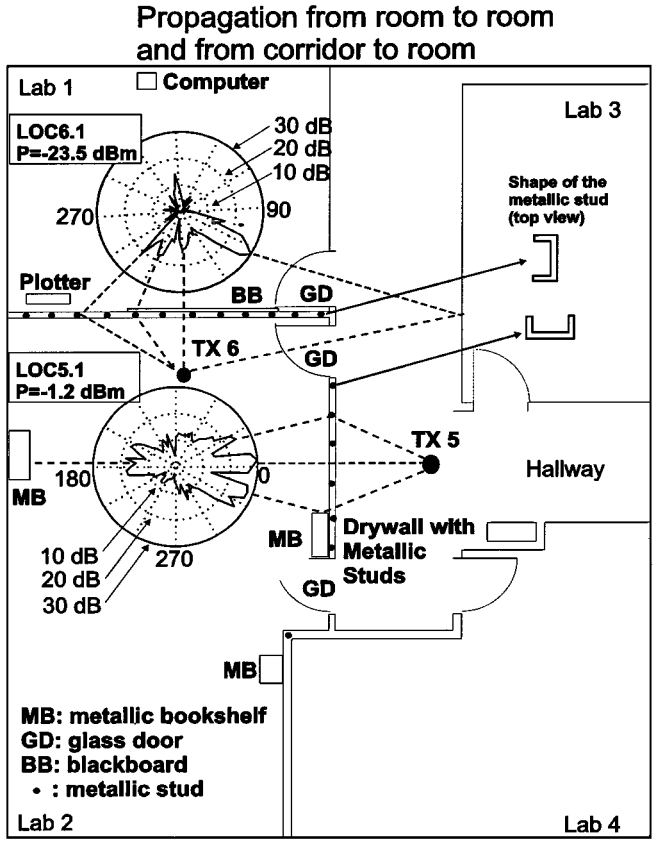

Fig. 6. AOA measurements for propagation into rooms (locations 5 and 6), relative power levels given in polar plots, and peak multipath power (P) given in text.

first-order reflections may be taken into consideration based on the site geometry. For more accurate predictions, ray-tracing with second-order or third-order reflections may be used.

- For NLOS applications, the direct path can be highly attenuated and become comparable to reflected multipath components. As a result, the multipath channel structure may become more diffuse than in LOS environments. When radio waves propagate through plasterboard walls, metallic studs within the wall must be considered. Penetration loss through the composite wall depends on the position and orientation of the studs within the wall. Results of penetration loss measurements are presented in Section IV-E. As shown in the measurement results from locations 5 and 6, reflection and scattering from the metallic studs may result in strong multipath components. More detailed analysis of the effects of different walls on short-path propagation can be found in [15] for 900 MHz, in [16] for 3.0 GHz, and [12], [17] for 60 GHz.

It is worth noting that millimeter-wave systems are mainly proposed for LOS applications. The measurement results and analysis show that site-specific propagation models, such as ray-tracing, can be used to precisely image the space-time channel for LOS applications.

IV. Statistical Parameters of the Channel

Site-specific prediction requires detailed knowledge of the propagation environments. When such information is not available, statistical models can be used to describe general channel properties which are useful for system design or for algorithm testing. This section presents the statistical parameters distilled from all the measurements in different locations. The measured parameters include received signal power, TOA parameters and AOA parameters.

A. Definition of the Statistical Parameters

Path Loss and Received Signal Power: The free-space *path loss* at a reference distance of d_0 is given by

$$PL_{fs}(d_0) = 20\log\left(\frac{4\pi d_0}{\lambda}\right) \quad (1)$$

where λ is the wavelength. Path loss over distance d can be described by the path loss exponent model as follows:

$$\overline{\mathrm{PL}}(d)[\mathrm{dB}] = PL_{fs}(d_0)\,(\mathrm{dB}) + 10n\log_{10}\left(\frac{d}{d_0}\right) \quad (2)$$

where $\overline{\mathrm{PL}}(d)$ is the average path loss value at a TR separation of d and n is the *path loss exponent* that characterizes how fast the path loss increases with the increase of TR separation. The path loss values represent the signal power loss from the transmitter antenna to the receiver antenna. These path loss values do not depend on the antenna gains or the transmitted power levels. For any given transmitted power, the received signal power can be calculated as

$$P_r(\mathrm{dBm}) = P_t(\mathrm{dBm}) + G_t(\mathrm{dB}) + G_r(\mathrm{dB}) - \overline{\mathrm{PL}}(d)(\mathrm{dB}) \quad (3)$$

where G_t and G_r are transmitter and receiver gains, respectively. In this measurement campaign, the transmitted power level was 25 dBm, the transmitter antenna gain was 6.7 dB, and the receiver antenna gain was 29 dB.

TOA Parameters: TOA parameters characterize the time dispersion of a multipath channel. The calculated TOA parameters include mean excess delay ($\bar{\tau}$), rms delay spread (σ_τ), and also timing jitter ($\delta(x)$) and standard deviation ($\Delta(x)$), in a small local area. Parameters of $\bar{\tau}$ and σ_τ are given as [6]

$$\bar{\tau} = \frac{\sum_{i=1}^{N} P_i\tau_i}{\sum_{i=1}^{N} P_i} \quad (4)$$

$$\sigma_\tau = \sqrt{\bar{\tau^2} - (\bar{\tau})^2} \quad (5)$$

$$\bar{\tau^2} = \frac{\sum_{i=1}^{N} P_i\tau_i^2}{\sum_{i=1}^{N} P_i} \quad (6)$$

where P_i and τ_i are the power and delay of the i_{th} multipath component of a PDP, respectively, and N is the total number of multipath components.

Timing jitter is calculated as the difference between the maximum and minimum measured values in a local area. Timing jitter $\delta(x)$ and standard deviation $\Delta(x)$ are defined as [13]

$$\delta(x) = \max_{i=1}^{M}\{x_i\} - \min_{i=1}^{M}\{x_i\} \quad (7)$$

$$\Delta(x) = \sqrt{\bar{x^2} - (\bar{x})^2} \quad (8)$$

$$\bar{x} = \sum_{i=1}^{M}\frac{x_i}{M} \quad (9)$$

$$\bar{x^2} = \sum_{i=1}^{M}\frac{x_i^2}{M} \quad (10)$$

where x_i is the measured value for parameter x ($\bar{\tau}$ or σ_τ) in the i_{th} measurement position of the spatial sampling and M is the total number of spatial samples in the local area. For example, for the track measurements, M was chosen to be 80.

Mean excess delay and rms delay spread are the statistical measures of the time dispersion of the channel. Timing jitter and standard deviation of $\bar{\tau}$ and σ_τ show the variation of these parameters over the small local area.

These TOA parameters directly affect the performance of high-speed wireless systems. For instance, the mean excess delay can be used to estimate the search range of rake receivers and the rms delay spread can be used to determine the maximum transmission data rate in the channel without equalization. The timing jitter and standard deviation parameters can be used to determine the update rate for a rake receiver or an equalizer.

AOA Parameters: AOA parameters characterize the directional distribution of multipath power. The recorded AOA parameters include angular spread Λ, angular constriction γ, maximum fading angle $\theta_{\max}$, and maximum AOA direction. Angular parameters Λ, γ and $\theta_{\max}$ are defined based on the Fourier transform of the angular distribution of multipath power, $p(\theta)$ [18]

$$\Lambda = \sqrt{1 - \frac{||F_1||^2}{||F_2||^2}} \quad (11)$$

$$\gamma = \frac{\left\|F_0F_2 - F_1^2\right\|}{||F_0||^2 - ||F_1||^2} \quad (12)$$

$$\theta_{\max} = \frac{1}{2}\mathrm{Phase}\left\{F_0F_2 - F_1^2\right\} \quad (13)$$

where

$$F_n = \int_0^{2\pi} p(\theta)\exp(jn\theta)d\theta. \quad (14)$$

F_n is the n_{th} Fourier transform of $p(\theta)$. As shown in [18], angular spread, angular constriction, and maximum fading angle are three key parameters to characterize the small scale fading behavior of the channel. These new parameters can be used for diversity techniques, fading rate estimation, and other space-time techniques. Maximum AOA provides the direction of the multipath component with the maximum power. It can be used in system installation to minimize the path loss. Detailed measured values of these parameters are presented in Section IV-B.

B. Results of Measured Statistical Parameters

A total of 8848 wideband PDPs and 94 PAPs were recorded in the eight locations, of which 2080 PDPs were recorded through linear track measurements and 6768 PDPs through spin measurements.

A summary of the measurements are presented in Table I for spin measurements and in Table II for linear track measurements. The presented parameters are averaged results from individual PDPs taken in a small local area. They represent the statistical temporal and spatial characteristics for the measured 60-GHz channels. Sections IV-C to IV-E provide details about AOA parameters, TOA parameters, and the received signal power.

1) AOA Statistics:

- *Angular distribution of multipath power*: Angular spread, Λ, characterizes the angular distribution of the multipath

TABLE I
SPIN MEASUREMENTS: TRANSMITTER–RECEIVER SEPARATIONS (TR) IN m, TIME DISPERSION PARAMETERS ($\bar{\tau}$ AND σ_τ) IN ns, ANGULAR DISPERSION PARAMETERS (Λ AND γ) ARE DIMENSIONLESS, MAXIMUM FADING ANGLE ($\theta_{\max}$) AND AOA OF MAXIMUM MULTIPATH ($\max AOA$) IN DEGREES, RATIO OF MAXIMUM MULTIPATH POWER TO AVERAGE POWER ($\mathrm{Peak}/\mathrm{Avg}$) IN dB AND MAXIMUM MULTIPATH POWER ($P_{\max}$) IN dBm

Site Info	#	TR	$\bar{\tau}$	σ_τ	Λ	γ	θ_{max}	$\frac{max}{AOA}$	$\frac{Peak}{Avg}$	P_{max}	Comments
	1.1	5	80.0	14.7	0.46	0.83	-80.7	-4.0	12.3	-14.9	
	1.2	10	52.0	18.8	0.44	0.74	-86.6	4.0	12.0	-18.2	
LOS,hallway	1.3	20	85.9	40.1	0.56	0.28	-61.9	8.0	14.5	-28.8	
Durham Hall	1.4	30	116.6	38.7	0.42	0.22	-66.4	5.0	14.7	-28.3	open area
	1.5	40	84.9	60.0	0.69	0.25	4.3	5.0	13.9	-38.2	
	1.6	50	52.1	26.1	0.66	0.26	8.2	10.0	13.3	-38.2	
	1.7	60	53.2	30.3	0.78	0.36	4.0	2.0	13.2	-40.8	
	2.1	5	51.0	20.7	0.48	0.88	-73.5	5.0	12.5	-13	
LOS,hallway	2.2	10	62.1	29.4	0.66	0.79	-72.3	21.0	11.4	-21.7	intersection
Whittemore	2.3	20	90.7	14.6	0.36	0.43	-73.8	4.0	12.9	-29.8	
	2.4	30	41.2	12.3	0.41	0.15	-64.8	10.0	13.8	-31.7	
	2.5	40	83.7	53.8	0.72	0.19	5.0	1.0	13.2	-36.0	
LOS, room	3.1	4.2	42.6	16.2	0.86	0.64	-79.2	0.0	12.5	-11.8	corner
Durham Hall	3.2	3.3	47.7	17.5	0.81	0.70	-79.1	5.0	13.1	-12.1	center
	4.1	7.1	46.6	13.0	0.84	0.55	-88.0	-60.0	12.3	-26.8	corner
LOS, room	4.2	3.8	64.3	13.3	0.62	0.74	-89.6	-1.0	13.1	-25.6	center
Whittemore	4.3	5.2	66.3	17.7	0.73	0.84	-35.2	49.0	14.0	-30.4	corner,$\perp$ to Tx
	4.4	4.2	77.8	13.3	0.78	0.72	-38.2	-49.0	14.2	-28.6	corner,$\perp$ to Tx
	5.1	2.4	49.1	21.4	0.81	0.13	-76.3	0.0	12.0	-6.0	LOS
Hallway to	5.2	2.4	41.6	18.1	0.74	0.44	-89.6	5.0	10.3	-14.1	through wall
room	5.3	2.4	95.8	14.6	0.63	0.40	-88.1	0.0	12.1	-5.6	LOS
	5.4	2.4	80.3	16.0	0.68	0.27	72.3	5.0	11.9	-8.9	through glass
Room to room	6.1	3	42.7	16.6	0.80	0.40	-25.3	52.0	11.5	-36.4	through wall
LOS, outdoor	7.1	1.9	41.3	17.4	0.12	0.97	-81.2	2.0	13.9	-15.0	Tx pattern
parking lot	7.2	1.9	56.6	16.1	0.49	0.94	-66.7	20.0	8.5	-29.9	Rx pattern
LOS, outdoor	8.1	2	24.4	7.7	0.26	0.76	-66.3	3.0	13.9	-10.1	near Durham Hall

power. It ranges from 0 to 1, with 0 indicating multipath coming from a single direction and 1 indicating no clear bias in the multipath AOA [18]. Measurement results show that the angular spread ranges from 0.36 to 0.78 for hallway measurements, 0.62 to 0.84 for room measurements, from 0.63 to 0.81 for indoor NLOS propagation, and 0.12 to 0.49 for outdoor measurements with few nearby obstructions. These measurement results show a clear increase of the angular spread from the least cluttered outdoor environments to obstructed NLOS indoor environments. In the hallway where multipath components are mainly constrained along the LOS path, the angular spread is smaller than that in rooms. Also, with the increase of distance along the hallway, the angular spread increases, indicating more multipath coming from different directions which have powers comparable to the LOS component. These angular spread values accurately reflect the correlation between the propagation environments and the multipath angle of arrival distributions.

- *Angular constriction*: Angular constriction γ indicates how multipath components are distributed along two directions. It ranges from 0 to 1, with 1 indicating multipath energy equally distributed in two directions. High angular constriction results were observed for close distances in the hallway and in the outdoor measurements near Durham Hall. This is the result of distribution of multipath energy between LOS and strong reflected wave components.
- *Maximum fading angle*: Maximum fading angle $\theta_{\max}$ shows the direction of the receiver motion required to achieve maximum fading rate. In the far side of the corridor (locations 1.6 and 1.7, for example), the received signal consists of an LOS path along the corridor and a reflected path from the end of corridor. These two components have opposite directions and thus the maximum fading angle is along the LOS path (close to 0°). In the near side of the corridor (such as locations 1.1 and 1.2), the main multipath components are from a LOS path and

TABLE II
TRACK MEASUREMENT RESULTS: TR SEPARATIONS (TR) IN m, TIME DISPERSION PARAMETERS ($\bar{\tau}$ AND σ_τ) IN ns, VARIATIONS OF TIME DISPERSION PARAMETERS ($\delta\bar{\tau}$, $\triangle\bar{\tau}$, $\delta\sigma_\tau$ AND $\triangle\sigma_\tau$) IN ns AND AVERAGE RECEIVED POWER (P_{rx}) IN dBm

Site Info	LOC #	TR	$\bar{\tau}$	σ_τ	$\delta\bar{\tau}$	$\triangle\bar{\tau}$	$\delta\sigma_\tau$	$\triangle\sigma_\tau$	P_r	Comments
	1.1	5	1.20	6.95	6.33	1.91	1.20	0.29	-13.7	
	1.2	10	6.16	5.88	5.06	1.20	6.16	1.73	-20.3	
LOS,hallway	1.3	20	32.61	47.25	32.89	8.43	32.61	9.02	-36.6	
Durham Hall	1.4	30	15.50	31.15	10.16	3.43	15.50	5.69	-31.2	open area
	1.5	40	27.60	37.04	25.89	8.81	27.60	9.76	-40.5	
	1.6	50	46.42	28.17	36.70	8.10	46.42	10.73	-42.8	
	1.7	60	6.38	22.57	5.99	1.82	6.38	1.57	-41.5	
	2.1	5	2.22	6.24	7.52	2.38	2.22	0.73	-16.7	
	2.2	10	2.78	6.48	8.24	2.61	2.78	0.82	-24.4	intersection
LOS,hallway	2.3	20	2.3	4.56	7.81	2.55	2.30	0.55	-32.86	
Whittemore	2.4	30	22.02	33.87	13.17	4.60	22.02	6.30	-34.7	
	2.5	40	77.3	45.07	105.04	34.41	77.30	25.86	-36.3	
LOS, room	3.1	4.2	0.74	4.85	6.20	1.88	0.74	0.20	-12.1	corner
Durham Hall	3.2	3.3	0.92	4.95	5.97	1.87	0.92	0.23	-12.9	center
	4.1	7.1	2.74	4.72	11.16	3.08	2.47	0.36	-29.7	corner
LOS, room	4.2	3.8	2.4	4.98	11.11	3.17	2.40	0.47	-24.2	center
Whittemore	4.3	5.2	12.88	31.10	26.36	6.86	12.88	2.95	-56.2	corner,$\perp$ to Tx
	4.4	4.2	21.3	33.94	31.5	7.4	21.3	5.43	-57.9	corner,$\perp$ to Tx
	5.1	2.4	0.83	5.50	2.41	0.69	0.83	0.32	-5.5	LOS
Hallway to	5.2	2.4	2.46	7.41	2.61	0.84	2.46	0.94	-14.3	through wall
room	5.3	2.4	0.71	5.36	1.30	0.41	0.71	0.25	-6.7	LOS
	5.4	2.4	1.16	5.19	1.85	0.61	1.16	0.36	-9.1	through glass
Room to room	6.1	3	10.67	14.72	23.07	6.62	10.67	1.30	-12.8	LOS
	6.2	3	14.82	21.78	34.30	8.57	14.82	3.37	-48.3	through wall
LOS,outdoor	8.1	2	7.63	24.59	10.24	2.66	7.63	1.75	-2.4	near Durham Hall

two reflected paths from the sidewalls. The maximum fading angle would be roughly perpendicular to the LOS path. The measurement results show maximum fading angles of -80° and -86° for locations 1.1 and 1.2 and 8.2° and 4.0° for locations 1.6 and 1.7, respectively. These results agree well with the expected values.

- *Direction of maximum multipath power*: Maximum AOA shows the arrival direction of the strongest multipath component at the receiver. Measurement results show strong dependence of the maximum AOA on the propagation environments. For all LOS locations, almost all maximum AOAs are close to the LOS path within $\pm 5^\circ$. In locations 6.3 and 6.4, the spin measurements were taken with the track orthogonal to the transmitter direction. The maximum AOAs are at 49° and -49°, which are the exact directions of the LOS paths. For NLOS locations, the maximum AOA is dependent on the specific propagation environments as discussed in Section III.
- *Peak to average power ratio*: Peak to average power ratio characterizes the power of strongest multipath as compared to the average received power from all directions. This ratio gauges the increase of the received signal power by pointing the directional antenna in the maximum AOA direction.
- *Peak multipath power*: Peak multipath power is the power level of the strongest multipath component as deduced from all the pointing angles of the receiver antenna. Received signal power level depends on the transmitter power level and the receiver attenuator settings. Therefore, the power level may change from location to location. We shall concern only the relative power for the same location. For hallway measurements at location 1, for example, the peak multipath power level decreases significantly with the increase of the separation at short distances. At large separation, such as at locations 1.5, 1.6, and 1.7, the peak multipath power remains almost constant. Similar trends were observed for the total received power. This indicates the waveguide effect of the long hallway. Detailed analysis on the received signal level is presented in Section IV-E.

2) TOA Statistics: Channel measurement results are highly dependent on the propagation environments and the

measurement system setup. Results from Tables I and II show a significant decrease of TOA delay statistics obtained from the track measurements compared to the spin measurements. For example, the mean excess delay from the track measurements in location 1.1 is only 1.2 ns, while it is 80.0 ns from the spin measurements. When transmitter and receiver antennas are aligned, such as track measurement at location 1.1, the main multipath component is the LOS component. Other multipath components are largely attenuated by the directional antenna, forcing the excess delay to be close to zero. However, if the antennas are not aligned and pointing into different directions, such as in spin measurements, the LOS path is attenuated and becomes comparable to the reflected multipath components, resulting in a significant increase of time delay parameters.

Therefore, for propagation research and system deployment, it is important to use channel propagation characteristics with consideration of the system setups. Table II provides channel parameters for systems with aligned antennas, while Table I presents results for systems with antennas pointing in arbitrary directions such as in a mobile environment.

Next, we summarize the measurement results from TOA measurements.

- RMS delay spread: When the receiver antenna is pointing into different directions, the delay spread is in the range of 7.5 ns to 76.46 ns for hallways and 10.89 ns to 41.01 ns for rooms. The measured delay spreads are in agreement with the measurement results in [19], where typical measured delay spreads for indoor 60-GHz channels range from 15 ns to 70 ns. When the receiver antenna is fixed, the delay spread is significantly smaller. Typical ranges are from 4.6 to 47.3 ns in the hallways and from 4.7 to 33.9 ns in the rooms.
- Mean excess delay: When the receiver antenna is rotating, the measured $\bar{\tau}$ is in the range of 41.2 to 116.6 ns for hallways, 42.6 to 77.8 ns for rooms, 41.6 to 91.8 ns for propagation from room to hallway and from room to room, and 24.4 to 56.3 ns for short distance outdoor measurements. In the hallway measurements, $\bar{\tau}$ increases significantly in the open area near the elevator, such as in location 1.4. Significant reduction of delay was also observed when the antennas were aligned and fixed.
- Timing jitter and standard deviation: Due to the small wavelength of 5 mm at 60 GHz, the radio channel may vary significantly within a small area (on the order of 20 wavelengths). Measurement results show high timing jitter and standard deviation for the measured excess delay and rms delay spread values of all locations. These results present a quantitative measure of the channel variations in a small local area.

3) Received Signal Power: Due to the high diffraction and penetration losses, the millimeter wave channel is mainly determined by LOS path and reflected paths. The received signal power largely depends on the antenna pattern, antenna alignment, and propagation environments. The maximum multipath power from the spin measurements shows the power level of the strongest multipath in all AOA directions. The average power presented in the track measurements shows the spatially averaged power with both antennas aligned. For the majority of the locations, the maximum multipath component has a power level that is higher than the averaged power. The trends of signal level changes are the same for both the maximum multipath power and the average received power. These trends are summarized as following:

- *Waveguide effects*: For hallway measurements, the received signal power decreased rapidly when the TR separation was increased from 2 to 20 m. After 20 m, the received signal power did not decrease appreciably with the increase of the distance. This trend was observed from both location 1 and location 2 hallway measurements. For instance, the received powers at locations 1.5, 1.6, and 1.7 were almost the same, although TR separation changed from 40 to 50 and 60 m, respectively. This is due to the waveguide effects of the radio wave propagation along the corridor at further separations. At small distances, the reflected wave components are rejected by the directional receiver antenna and waveguide effect is not dominant. However, at long distances, reflected wave components are close to the LOS path and are received by the receiver antenna. The total received field is stronger than it should be from free space propagation and the transmitted wave propagates in a guided fashion. The interplay of the antenna pattern, site geometry and reflected wave components can be explained using the power zone theory [20].
- *Antenna effects and power zone theory*: When directional antennas are used, the majority of the radiated energy is concentrated along the LOS path. Power zone plots are developed to characterize the power concentration. When TR separation is relatively small, no obstacles intersect the power zones. And, therefore, the received signal power is mainly from LOS path. As a result, with an increase in distance, the received signal power decreases with a path loss exponent close to 2. However, when TR separation is large, sidewalls of the hallway and the floor are close to the main power zone and reflected power contributes to the total received power. The received signal consists of both LOS component and reflected components along the corridor.
- *Penetration losses*: Measurements through glass door and interior walls in locations 5 and 6 showed power losses of 8.8 and 35.5 dB through two composite walls and a loss of 2.5 dB through a glass door. These results indicate that the quantity and position of the metallic studs within the composite wall are important factors to determine the penetration loss. When the studs are not blocking the transmission path, the penetration loss is 8.8 dB, comparable to the loss through a plasterboard wall [17]. When the stud is blocking the transmission path, the penetration loss is 35.5 dB, comparable to the loss through a concrete wall [12], [21]. Rule-of-thumb penetration loss values are presented in Table III.
- Scatter plot of path loss values: The total path loss from the transmitter to the receiver was calculated from the measurement results. The scatter plot is presented in Fig. 7. As shown in Fig. 7, for LOS propagation, the path loss values are close to the free-space path loss values. For NLOS propagation, high penetration loss values can result in high

TABLE III
MEASURED PENETRATION LOSSES AND RESULTS FROM LITERATURE

Material	Penetration loss	Ref.
Composite wall with studs not in the path	8.8	
Composite wall with studs in the path	35.5 dB	
Glass door	2.5 dB	
Concrete wall 1 week after concreting	73.6 dB	[12]
Concrete wall 2 weeks after concreting	68.4 dB	[12]
Concrete wall 5 weeks after concreting	46.5 dB	[12]
Concrete wall 14 months after concreting	28.1 dB	[12]
Plasterboard wall	5.4 to 8.1 dB	[17]
Partition of glass wool with plywood surfaces	9.2 to 10.1 dB	[17]
Partition of cloth-covered plywood	3.9 to 8.7 dB	[17]
Granite with width of 3 cm	>30 dB	[21]
Glass	1.7 to 4.5 dB	[21]
Metalized glass	> 30 dB	[21]
Wooden panels	6.2 to 8.6 dB	[21]
Brick with width of 11 cm	17 dB	[21]
Limestone with width of 3 cm	> 30 dB	[21]
Concrete	> 30 dB	[21]

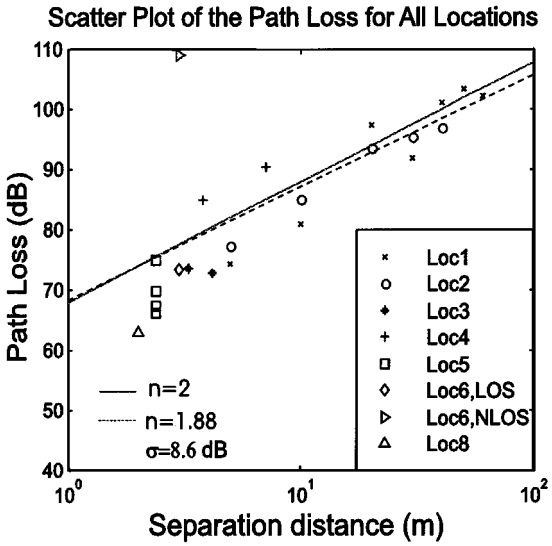

Fig. 7. Scatter plot of the measured path loss values.

path loss values. For example, in location 6, the path loss value is as high as 108 dB. This is caused by the 35.5-dB penetration loss through the composite wall.

V. SUMMARY

This work presents an extensive measurement campaign and a detailed analysis of the 60-GHz space-time channel. Multipath components were resolved in space by sweeping a directional antenna and in time by using a spread spectrum sliding correlator system. Measurement results include PDPs, PAPs, received signal power, AOA parameters, and TOA parameters. The PAPs are analyzed in context with site-specific information. Results show strong correlation between the multipath distribution and the propagation environments. Ray tracing of first-order and second-order reflections seems to be sufficient for channel prediction for LOS applications. Metallic furniture and objects must be considered in the ray tracing model. Measurements through composite walls show that the wall structure can be a crucial factor in determining signal power level as well as multipath structure. Statistical parameters, such as angular spread, peak AOA, and maximum fading rate angle were measured and related to the multipath models. The measured power, AOA, and TOA parameters agree well with the theoretical expectations. These measurement results not only present important empirical values for 60-GHz system design and a fundamental basis for ray tracing development and verification, but also provide a better understanding of the radio wave propagation at millimeter-wave frequencies.

ACKNOWLEDGMENT

The authors would like to thank Dr. J. Schaffner for his invaluable contribution in designing the measurement system and Dr. G. Durgin, E. Lao, B. Henty, J. Aron, and Dr. P. Cardieri for their great assistance in the measurement campaign. Thanks are also due to the anonymous reviewers for their insightful technical comments.

REFERENCES

[1] R. H. Clark, "A statistical theory of mobile-radio reception," *Bell System Tech. J.*, vol. 47, pp. 957–1000, 1968.
[2] M. J. Gans, "A power-spectral theory of propagation in the mobile radio environment," *IEEE Trans. Veh. Technol.*, vol. VT-20, pp. 27–38, Feb. 1972.
[3] R. B. Ertel, P. Cardieri, K. W. Sowerby, T. S. Rappaport, and J. H. Reed, "Overview of spatial channel models for antenna array communication systems," *IEEE Pers. Commun. Mag.*, vol. 5, pp. 10–12, Feb. 1998.
[4] J. C. Liberti and T. S. Rappaport, *Smart Antennas for Wireless Communications: IS-95 and Third Generation CDMA Applications*. Englewood Cliffs, NJ: Prentice-Hall, 1999.
[5] P. Charriere, K. H. Craig, and A. Seville, "A ray-based, millimeter wave urban propagation tool," in *Proc. ICAP, IEE Conf. Pub 407*, Apr. 1995, pp. 258–261.
[6] T. S. Rappaport, *Wireless Communications: Principles and Practice*. Englewood Cliffs, NJ: Prentice-Hall, 1996.
[7] J. Litva, A. Ghaforian, and V. Kezys, "High-resolution measurements of AOA and time-delay for characterizing indoor propagation environments," in *Proc. 8th Int. Conf. Wireless Communications*, vol. 2, Calgary, Canada, July 1996, pp. 514–518.
[8] J. Fuhl, J. P. Rossi, and E. Bonek, "High-resolution 3-D direction-of-arrival determination for urban mobile radio," *IEEE Trans. Antennas Propagat.*, vol. 45, pp. 672–671, Apr. 1997.
[9] J. P. Rossi, J. P. Barbot, and A. J. Levy, "Theory and measurement of the angle of arrival and time delay of UHF radiowave using a ring array," *IEEE Trans. Antennas Propagat.*, vol. 45, pp. 876–884, May 1997.
[10] Y. L. C. de Jong and M. H. A. J. Herben, "High-resolution angle-of-arrival measurement of the mobile radio channel," *IEEE Trans. Antennas Propagat.*, vol. 47, pp. 1677–1687, Nov. 1999.
[11] H. Droste and G. Kadel, "Measurement and analysis of wideband indoor propagation characteristics at 17 GHz and 60 GHz," in *Proc. IEE Antennas Propagation, Conf. (Publication no. 407)*, Apr. 1995, pp. 288–291.
[12] T. Manabe, Y. Miura, and T. Ihara, "Effects of antenna directivity and polarization on indoor multipath propagation characteristics at 60 GHz," *IEEE J. Select. Areas Commun.*, vol. 14, pp. 441–448, Apr. 1996.
[13] G. D. Durgin, V. Kukshya, and T. S. Rappaport, "Wideband measurements of angle and delay dispersion for outdoor and indoor peer-to-peer radio channels at 1920 MHz," *IEEE Trans. Antennas Propagat.*, submitted for publication.
[14] A. D. Yaghjian, "Approximate formulas for the far field and gain of open-ended rectangular waveguide," *IEEE Trans. Antennas Propagat.*, vol. AP-32, pp. 378–384, Apr. 1984.

[15] C. L. Holloway, P. L. Perini, R. R. Delyzer, and K. C. Allen, "Analysis of composite walls and their effects on short-path propagation modeling," *IEEE Trans. Veh. Technol.*, vol. 46, pp. 730–738, Aug. 1997.
[16] W. Honcharenko and H. Bertoni, "Transmission and reflection characteristics at concrete block walls in the UHF bands proposed for future PCS," *IEEE Trans. Antennas Propagat.*, vol. 42, pp. 232–239, Feb. 1994.
[17] K. Sato, T. Manabe, T. Ihara, H. Saito, S. Ito, T. Tanaka, K. Sugai, N. Ohmi, Y. Murakami, M. Shibayama, Y. Konishi, and T. Kimura, "Measurements of reflection and transmission characteristics of interior structures of office building in the 60-GHz band," *IEEE Trans. Antennas Propagat.*, vol. 45, pp. 1783–1792, Dec. 1997.
[18] G. Durgin and T. S. Rappaport, "Theory of multipath shape factors for small-scale fading wireless channels," *IEEE Trans. Antennas Propagat.*, vol. 48, pp. 682–693, May 2000.
[19] P. Smulders and L. Correia, "Characterization of propagation in 60 GHz radio channels," *Electron. Commun. Eng. J.*, pp. 73–80, Apr. 1997.
[20] H. Xu, T. S. Rappaport, R. J. Boyle, and J. Schaffner, "Measurements and modeling for 38-GHz point-to-multipoint radiowave propagation," *IEEE J. Select. Areas Commun.*, vol. 18, pp. 310–321, Mar. 2000.
[21] B. Langen, G. Lober, and W. Herzig, "Reflection and transmission behavior of building materials at 60 GHz," in *Proc. IEEE PIMRC'94*, Hague, Netherlands, Sept. 1994, pp. 505–509.
[22] H. Xu, V. Kukshya, and T. Rappaport, "Spatial and temporal characterization of 60 GHz channels," in *Proc. IEEE VTC'2000*, Boston, MA, Sept. 24–28, 2000.

Hao Xu (S'96–M'00) was born in Wuhan, China, on February 28, 1971. He received the B.S. and M.S. degrees from Moscow Power Engineering Institute and Technical University, Moscow, Russia in 1994 and 1996, respectively. He received the Ph.D. degree from Virginia Polytechnic Institute and State University, Blacksburg, VA, in 2000.

From 1996 to 2000, he worked as a Research Assistant in the Mobile and Portable Radio Research Group (MPRG), Virginia Polytechnic Institute and State University while pursuing his Ph.D. He joined Wireless Communications Research Department at Bell Laboratories, Crawford Hill, in 2000. His current research interests include MIMO channel characterization and standardization of MIMO channel model for third-generation wireless systems as well as adaptive antenna techniques and advanced receiver design.

Dr. Xu received the IEEE Communications Society Stephen O. Rice Prize Paper Award in 1999. He also received the Zhang Zhongzhi Price Award from the University of Science and Technologies in China (USTC) in 1989. He is a member of Eta Kappa Nu and Sigma Xi Scientific Research Society.

Vikas Kukshya (M'99) was born in Lucknow, India, on November 19, 1975. He received the Bachelor of Engineering (B.E.) degree in electronics and communications from Gujarat University, India, in 1997 and the M.S. degree in Electrical Engineering from Virginia Polytechnic Institute and State University, Blacksburg, VA, in June 2001.

In 1996, Vikas worked at Space Applications Center (SAC), Indian Space Research Organization (ISRO), as a Project Trainee. He designed, implemented, and evaluated the performance of a single board computer (SBC) for altimeter and scatterometer applications aboard the "OCEANSAT" satellite system. From 1997 to 1999, Vikas worked for Tata Telecom Limited, a joint venture company of Tata and Avaya (former Lucent Technologies). From 1999 to 2001, he worked as a Research Assistant to Dr. Theodore S. Rappaport at Mobile and Portable Radio Research Group (MPRG), Virginia Polytechnic Institute. Since June 2001, he has been with HRL Laboratories and specializes in wideband free-space optical and millimeter wave propagation measurements.

Dr. Kukshya was awarded a Merit medal by the Institution of Engineers, India, for academic excellence and was awarded merit certificates by the Vice President and Managing Director of Tata Telecom Limited for excellent performance.

Theodore S. Rappaport (S'83–M'84–S'85–M'87–SM'90–F'98) received B.S.E.E., M.S.E.E., and Ph.D. degrees from Purdue University, Lafayette, IN, in 1982, 1984, and 1987, respectively.

Since 1988, he has been on the Virginia Polytechnic Institute and State University Electrical and Computer Engineering faculty, where he is the James S. Tucker Professor and founding director of the Mobile & Portable Radio Research Group (MPRG), a university research and teaching center dedicated to the wireless communications field. In 1989, he founded TSR Technologies, Inc., a cellular radio/PCS manufacturing firm that he sold in 1993. He has 22 patents issued or pending and has authored, coauthored, and coedited 17 books in the wireless field, including the popular textbook *Wireless Communications: Principles & Practice* (Englewood Cliffs, NJ: Prentice-Hall, 1996), *Smart Antennas for Wireless Communications: IS-95 and Third Generation CDMA Applications* (Englewood Cliffs, NJ: Prentice-Hall, 1999), and several compendia of papers, including *Cellular Radio & Personal Communications: Selected Readings* (Piscataway, NJ: IEEE Press, 1995), *Cellular Radio & Personal Communications: Advanced Selected Readings* (Piscataway, NJ: IEEE Press, 1996), and *Smart Antennas: Selected Readings* (Piscataway, NJ: IEEE Press, 1998). He has coauthored more than 150 technical journal and conference papers. Since 1998, he has been series editor for the Prentice-Hall *Communications Engineering and Emerging Technologies* book series. He serves on the editorial board of *International Journal of Wireless Information Networks* (New York, NY: Plenum), and the advisory board of *Wireless Communications and Mobile Computing* for Wiley InterScience. He is also Chairman of Wireless Valley Communications, Inc., a microcell and in-building design and management product company. He is a Registered Professional Engineer in the state of Virginia. He has consulted for over 25 multinational corporations and has served the International Telecommunications Union as a consultant for emerging nations.

Dr. Rappaport received the Marconi Young Scientist Award in 1990, an NSF Presidential Faculty Fellowship in 1992, and the Sarnoff Citation from the Radio Club of America in 2000. He was recipient of the 1999 IEEE Communications Society Stephen O. Rice Prize Paper Award and is active in the IEEE Communications and Vehicular Technology Societies. He is a Fellow and past member of the board of directors of the Radio Club of America.